J. Phys. Chem. A **2001,** *105,* 602−613

Theoretical Estimation of Lithium Isotopic Reduced Partition Function Ratio for Lithium Ions in Aqueous Solution

Kazuyo Yamaji, Yoji Makita, Hidekazu Watanabe, Akinari Sonoda, Hirofumi Kanoh,* Takahiro Hirotsu, and Kenta Ooi*

Shikoku National Industrial Research Institute, 2217-14 Hayashi-cho, Takamatsu 761-0395, Japan

Received: April 4, 2000; In Final Form: August 8, 2000

The reduced partition function ratio for lithium ions in an aqueous solution is derived from the extrapolation of the values of the reduced partition function ratio (f_n^{r}) of hydrated lithium ion clusters $[\mathrm{Li(H_2O)}_n]^+$ up to $n = 6$. In $[\mathrm{Li(H_2O)}_n]^+$ clusters, the f_n^{r} values can be calculated from the normal vibration frequencies according to Bigeleisen and Mayer's theory. To obtain the values of f_n^{r}, the normal vibration frequency calculations were carried out for optimized structures of $[\mathrm{Li(H_2O)}_n]^+$ ($n = 1-6$) using the RHF/6-31+G(d), RHF/6-31++G(d,p), RHF/6-311+G(d) and MP2/6-31+G(d) methods by means of the ab initio molecular orbital method. All of those structures having high symmetry were confirmed to have real harmonic frequencies at the RHF/6-31+G(d) and RHF/6-31++G(d,p) levels. For the two RHF methods, the value of f_n^{r} increases to about 1.07 with an increase of the hydration number n, and reaches maximum at $n = 4$. In the most stable isomers of $[\mathrm{Li(H_2O)}_n]^+$ clusters for $n = 5$ and 6, respectively, the first hydration shell is saturated with the four water molecules, and the size dependence of the f_n^{r} values converges for $n \geq 4$. The converged value 1.07 can, therefore, be regarded as the reduced partition function ratio for lithium ions in aqueous solution, and gives the upper limit of the isotopic separation factor in an aqueous solution−exchanger system.

Introduction

The lithium element has two stable naturally occurring isotopes whose mass numbers are 6 and 7. They can be expected to have large isotopic fractionations because of their large difference in relative masses. Moreover, the study of lithium isotopic fractionation is important, not only for industrial nuclear science, but also for fundamental material and geological science. The lithium isotopic fractionations through chemical exchanges between the two phases have been studied in various systems such as lithium amalgam, lithium metal, organic, and inorganic ion exchangers, macrocyclic polyether, and membranes.[1−8] The highest isotopic fractionation ability was obtained in the lithium isotopic exchange reaction between an aqueous solution phase and an amalgam phase, where the separation factor was 1.05.[2]

The lithium isotopic exchange reaction between an aqueous solution phase (aq) and an exchanger phase (exch) can be written as

$$^{6}\mathrm{Li}^{+}_{\mathrm{aq}} + {}^{7}\mathrm{Li}^{+}_{\mathrm{exch}} \overset{S}{\rightleftharpoons} {}^{7}\mathrm{Li}^{+}_{\mathrm{aq}} + {}^{6}\mathrm{Li}^{+}_{\mathrm{exch}} \tag{1}$$

where the value of S, called the separation factor, is the equilibrium constant of the isotopic exchange reaction shown in eq 1. The value of S can be expressed using partition function ratios as follows:[9,10]

$$S = \frac{[{}^{7}\mathrm{Li}^{+}/{}^{6}\mathrm{Li}^{+}]_{\mathrm{aq}}}{[{}^{7}\mathrm{Li}^{+}/{}^{6}\mathrm{Li}^{+}]_{\mathrm{exch}}} = \frac{(s^{7}/s^{6})_{\mathrm{aq}} \cdot f_{\mathrm{Li,aq}}}{(s^{7}/s^{6})_{\mathrm{exch}} f_{\mathrm{Li,exch}}} \tag{2}$$

where $f_{\mathrm{Li,aq}}$ and $f_{\mathrm{Li,exch}}$ are the partition function ratios of the lithium species in phases of an aqueous solution and an exchanger, respectively, and $(s^7/s^6)_{\mathrm{aq}}$ and $(s^7/s^6)_{\mathrm{exch}}$ are the ratios of the symmetry numbers of the lithium isotopes in the two phases. In the present case, these ratios are equal to unity since the lithium atom is located at the center of the symmetry axis of the molecules. Moreover, S can be given using reduced partition function ratios:

$$S = \frac{f^{\mathrm{r}}_{\mathrm{Li,aq}}}{f^{\mathrm{r}}_{\mathrm{Li,exch}}} \tag{3}$$

where $f^{\mathrm{r}}_{\mathrm{Li,aq}}$ and $f^{\mathrm{r}}_{\mathrm{Li,exch}}$ are the reduced partition function ratios of the lithium species in phases of an aqueous solution and an exchanger, respectively.

The isotopic effect does not appear in the classical expression. In quantum mechanics, a partition function can be written as a product of translational, rotational, and vibrational partition functions in the first approximation. The reduced partition function ratio (f^{r}) is $f^{\mathrm{r}} = f_{\mathrm{qm}}/f_{\mathrm{cl}}$, where f_{qm} and f_{cl} is the partition function ratios calculated using the quantum-mechanical expression and classical expression, respectively. The translational partition function is equal to the classical one at all temperatures. The rotational partition function in all cases except hydrogen is classical at room temperature. Thus, the isotopic effect arises mainly from the difference between the vibration energies of the lithium isotopic species. The value of f^{r} can be experimentally calculated with a Raman active spectrum using a rough approximate formula derived by Bigeleisen and Mayer.[10] However, it has proven very difficult to experimentally estimate a reasonable $f^{\mathrm{r}}_{\mathrm{Li,aq}}$ value for the lithium ion in diluted solution, although Raman spectroscopy for hydrated lithium ions has been

---

* To whom correspondence should be addressed. E-mail: kano@sniri.go.jp. E-mail: ooi@sniri.go.jp.

10.1021/jp001303i CCC: $20.00

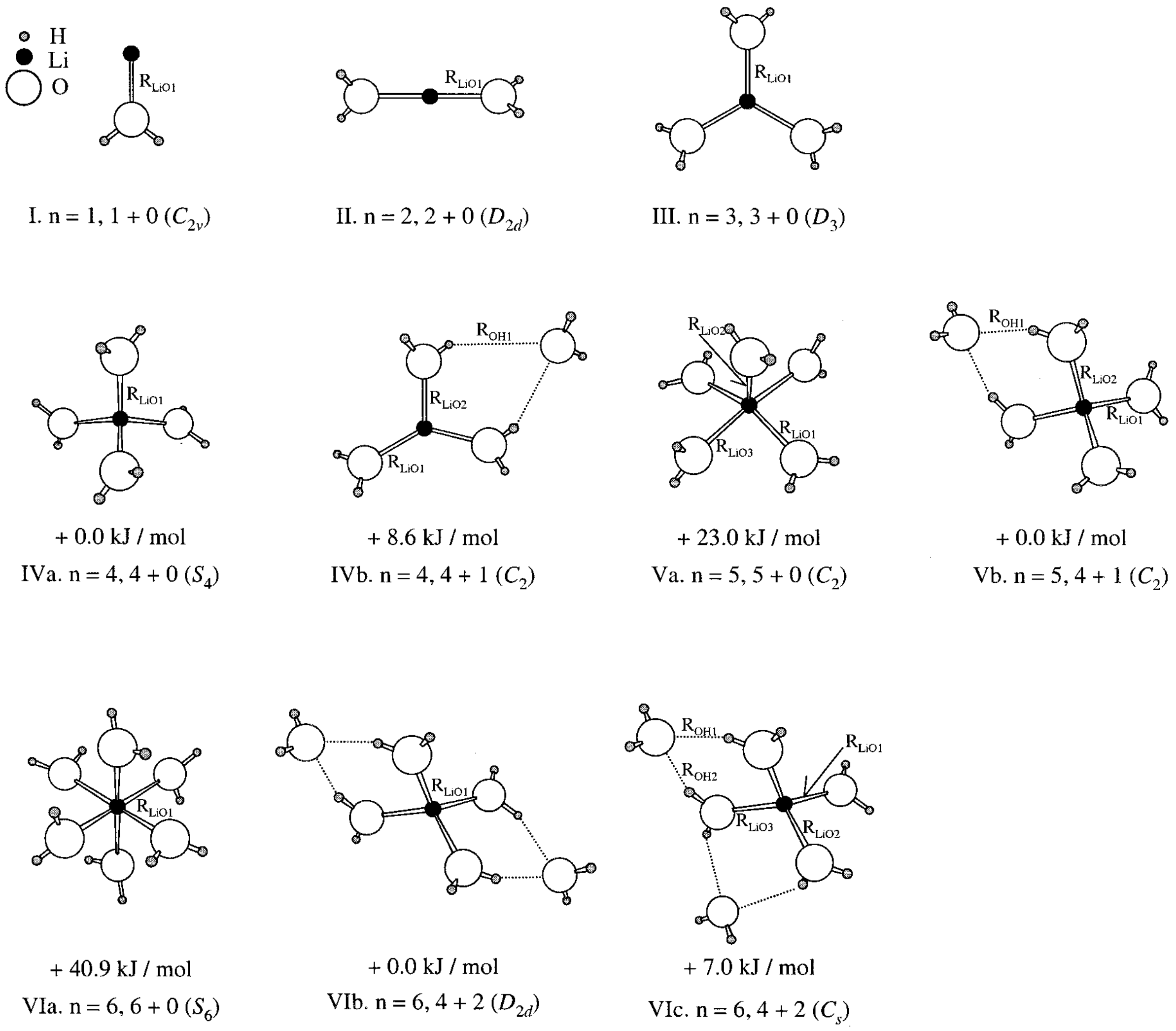

I. n = 1, 1 + 0 (C_{2v})

II. n = 2, 2 + 0 (D_{2d})

III. n = 3, 3 + 0 (D_3)

+ 0.0 kJ / mol
IVa. n = 4, 4 + 0 (S_4)

+ 8.6 kJ / mol
IVb. n = 4, 4 + 1 (C_2)

+ 23.0 kJ / mol
Va. n = 5, 5 + 0 (C_2)

+ 0.0 kJ / mol
Vb. n = 5, 4 + 1 (C_2)

+ 40.9 kJ / mol
VIa. n = 6, 6 + 0 (S_6)

+ 0.0 kJ / mol
VIb. n = 6, 4 + 2 (D_{2d})

+ 7.0 kJ / mol
VIc. n = 6, 4 + 2 (C_s)

Figure 1. Optimized structures of $[Li(H_2O)_n]^+$ for $n = 1-6$ calculated at the RHF/6-31+G(d) and RHF/6-31++G(d,p) levels. Their point groups are given in parentheses. Geometrical parameters are given in Table 1. For structures of $n = 5$ and 6, the relative energy differences (kJ/mol) between isomers are also given under each structure calculated at the RHF/6-31+G(d) level.

extensively studied by several authors.[11-14] Raman active spectrum data obtained so far do not inspire confidence because these measurements vary largely in the literature, with values changing greatly depending on the concentration of the solution and the kind of counteranion. Even in diluted solution, the obtained spectra vary widely depending on counteranions of various lithium salts (for example, LiCl or LiBr), whose influence cannot be completely removed.

A computer simulation is a powerful method to estimate the value of $f^r_{Li,aq}$ in the diluted solution. Recent developments in computer chemistry enable us to simulate the stable structure of hydrated lithium ions and their vibration analysis. The static and dynamic structures of hydrated lithium ions have been extensively studied with Monte Carlo (MC), molecular dynamics (MD), and the ab initio molecular orbital (MO) methods.[14-21] The isotopic effect can easily be investigated with normal frequency analysis, which is carried out by means of the ab initio MO method.

In the present paper, we tried to estimate the value of $f^r_{Li,aq}$ using the ab initio MO calculation. At first, structures of $[Li(H_2O)_n]^+$ clusters up to $n = 6$ were fully optimized, and the normal vibration analysis was carried out at the optimized geometry. Next, the values of f^r_n for $[Li(H_2O)_n]^+$ clusters ($n = 1-6$) were calculated from differences between the obtained normal frequencies for each lithium isotopic species using Bigeleisen and Mayer's approximate formula.[10] Finally, the value of $f^r_{Li,aq}$ was estimated from the trend of the size dependence on the values of f^r_n for $[Li(H_2O)_n]^+$ clusters ($n = 1-6$). Furthermore, when the lithium atom was symmetrically surrounded by n identical oxygen atoms or water molecules, the reduced partition function ratios of $[Li(H_2O)_n]^+$ clusters ($n = 2-6$) could be approximately evaluated from only a totally symmetric stretching frequency for a central lithium atom by Bigeleisen and Mayer's rough approximate formula,[10] whose validity was confirmed.

Theoretical Basis

According to the theory of Bigeleisen and Mayer,[10] f^r can be given as follows:

$$f^r = \frac{Q_{vib}{}^{^7Li}\Pi_i u_i{}^{^7Li}}{Q_{vib}{}^{^6Li}\Pi_i u_i{}^{^6Li}} \tag{4}$$

where the Born−Oppenheimer approximation, classical approximations for translational and rotational motions, and the harmonic oscillator approximation are used. Then, $Q_{vib}{}^{^7Li}$ and $Q_{vib}{}^{^6Li}$ are the vibrational partition functions for the molecules with two isotopes, ^7Li and ^6Li, respectively. If the explicit

TABLE 1: Optimized Structural Parameters (angstroms)[a] and Hydration Energies $-\Delta E_n$ (kJ/mol), Relative Energy Differences Δe_n (kJ/mol) between Isomers

symbol	symmetry	level[b]	R_{LiO_1}	R_{LIO_2}	R_{LiO_3}	R_{OH_1}	R_{OH_2}	$-\Delta_n$[c]	Δe_n
I (1+0)	C_{2v}	A	1.850					153.6	
		B	1.849					151.5	
		C	1.839					164.2	
		D	1.874					153.0	
II (2+0)	D_{2d}	A	1.878					135.4	
		B	1.875					133.7	
		C	1.867					144.1	
		D	1.902					138.1	
III (3+0)	D_3	A	1.915					102.9	
		B	1.915					101.1	
		C	1.902					111.1	
		D	1.942					107.0	
IVa (4+0)	S_4	A	1.969					73.7	
		B	1.969					72.3	
		C	1.956					79.5	
IVb (3+1)	C_2	A	1.901	1.920		2.036		65.1	8.6
		B	1.898	1.920		2.061		62.4	9.9
		C	1.890	1.904		2.021		69.9	9.7
		D	1.913	1.931		1.941		79.1	
Va (5+0)	C_2	A	2.007	2.023	2.173			37.0	23.0
		B	2.004	2.025	2.192			34.0	23.1
		C	1.984	2.005	2.170			41.6	22.7
Vb (4+1)	C_2	A	1.965	1.967		2.041		60.0	
		B	1.962	1.968		2.067		57.0	
		C	1.962	1.967		2.076		64.3	
		D	1.965	1.973		1.950			
VIa (6+0)	S_6	A	2.150					38.0	40.9
		B	2.158					33.7	43.2
		D	2.130						27.8
VIb (4+2)	D_{2d}	A	1.967			2.052		55.9	
		B	1.965			2.079		53.9	
		C	1.952			2.041		60.9	
		D	1.970			1.960			
VIc (4+2)	C_s	A	1.949	1.971	1.980	2.045	2.094	48.9	7.0
		B	1.948	1.972	1.977	2.070	2.128	46.5	7.3
		C	1.939	1.955	1.963	2.037	2.086	52.8	8.1
		D	1.960	1.970	1.988	1.964	1.983		5.4

[a] Parameters are shown in Figure 1. [b] A: RHF/6-31+G(d).B: RHF/6-31++G(d,p). C: RHF/6−311+G(d) D: MP2/6-31+G(d). [c] $-\Delta E_n = E_{[Li(H_2O)_n]^+} - E_{[Li(H_2O)_{n-1}]^+} - E_{H_2O}$. For VIa, using a total energy of Va for $E_{[Li(H_2O)_{n-1}]^+}$. For VIb and VIc, using a total energy of Va for $E_{[Li(H_2O)_{n-1}]^+}$.

expression for Q_{vib} is substituted in eq 4, the value of f^r is calculated as

$$f^r = \Pi_i \frac{\exp(-u_i^{7Li}/2)\{1 - \exp(-u_i^{6Li})\}\, u_i^{7Li}}{\exp(-u_i^{6Li}/2)\{1 - \exp(-u_i^{7Li})\}\, u_i^{6Li}} \tag{5}$$

where u_i ($u_i = h\nu_i/kT$) is calculated from the normal vibration frequency ν_i, h is Plank's constant, k is Boltzmann's constant, and u_i^{7Li} and u_i^{6Li} are the values for ^{7}Li and ^{6}Li, respectively. Thus, f^r can be estimated through the calculation of the normal vibrations of molecules with the isotopes.

Furthermore, when the central isotopic lithium atom of mass M or M + ΔM is symmetrically surrounded by n identical oxygen atoms of mass m, f^r can be approximately calculated from Bigeleisen and Mayer's rough approximate formula shown in eq 6.

$$f^r \simeq f^{r,a} = 1 + \frac{\Delta M m}{24M(M + \Delta M)} u_1^2 n \tag{6}$$

where u_1 is calculated from the totally symmetric stretching frequency ν_1 of the bond between the central atom and the surrounding atoms, which is usually known from Raman active spectra.

Computational Method

Geometric structures of $[Li(H_2O)_n]^+$ up to $n = 6$ were determined with the ab initio MO method. The optimization was carried out with the RHF/6-31+G(d), RHF/6-31++G(d,p), RHF/6-311+G(d) and MP2/6-31+G(d) methods of approximation. To confirm the true local minimum, normal frequencies were evaluated at every optimized structure. The value of the reduced partition function ratio for each cluster was derived from the calculated normal frequencies with the RHF/6-31+G(d) and RHF/6-31++G(d,p) methods. To discuss the normal frequencies, the scaling factors, 0.8965 and 0.8841 were applied to the values obtained from the RHF/6-31+G(d) and RHF/6-31++G(d,p) methods, respectively. The values of the scaling factors were determined with three modes of free water molecules by

TABLE 2: Normal Vibration Frequencies $\tilde{\nu}$ (cm^{-1}) of $[Li(H_2O)_1]^+$ with ^{6}Li and ^{7}Li Using Various Calculation Methods I: $n = 1$, 1 + 0 (C_{2v}), $\Gamma_{vib} = 3A_1 + 2B_1 + B_2$

	method[a]					
	A			B		
mode[b]	$\tilde{\nu}_{^6Li}$	$\tilde{\nu}_{^7Li}$	$\Delta\tilde{\nu}$[c]	$\tilde{\nu}_{^6Li}$	$\tilde{\nu}_{^7Li}$	$\Delta\tilde{\nu}$[c]
B_1	400	399	1	409	408	1
B_2	526	524	2	505	502	3
A_1	529	500	29	520	491	29
A_1	1653	1653	−	1589	1589	
A_1	3594	3594	−	3608	3608	
B_2	3669	3669	−	3684	3684	

[a] These various calculation methods are (A) RHF/6-31+G(d) and (B) RHF/6-31++G(d,p), scaled by 0.8964 and 0.8841, respectively. [b] Schematic representations of normal vibration modes are shown. [c] Values give differences of frequencies for two isotopes.

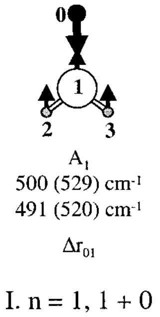

Figure 2. Schematic representations of normal vibration mode having a lithium isotopic shift for $[Li(H_2O)_1]^+$. The wave numbers (upper line, calculated by the RHF/6-31+G(d) level; lower line, calculated by the RHF/6-31++G(d,p) level), are the data for ^{7}Li (the data for ^{6}Li) after scaling each value (0.8964 for the RHF/6-31+G(d) level, 0.8841 for the RHF/6-31+G(d) level). The vibration mode represented by the internal coordinates is given under the model.

TABLE 3: Normal Vibration Frequencies $\tilde{\nu}$ (cm^{-1}) of $[Li(H_2O)_2]^+$ with ^{6}Li and ^{7}Li Using Various Calculation Methods II: $n = 2, 2 + 0$ (D_{2d}), $\Gamma_{vib} = 3A_1 + B_1 + 3B_2 + 4E$

	method[a]					
	A			B		
mode[b]	$\tilde{\nu}_{^6Li}$	$\tilde{\nu}_{^7Li}$	$\Delta\tilde{\nu}^c$	$\tilde{\nu}_{^6Li}$	$\tilde{\nu}_{^7Li}$	$\Delta\tilde{\nu}^c$
E	56	53	3	65	61	4
B_1	76	76		64	64	
A_1^d	251	251		246	246	
E	368	367	1	378	377	
E	505	502	3	485	482	3
B_2	641	601	40	627	588	39
B_2	1647	1647		1582	1582	
A_1	1648	1648		1583	1583	
B_2	3604	3604		3617	3617	
A_1	3607	3607		3619	3619	
E	3685	3685		3698	3698	

[a] These various calculation methods are (A) RHF/6-31+G(d) and (B) RHF/6-31++G(d,p), scaled by 0.8964 and 0.8841, respectively. [b] Schematic representations of normal vibration modes are shown. [c] Values give differences of frequencies for two isotopes. [d] Values for A_1 show mode for totally symmetric stretching of Li−O.

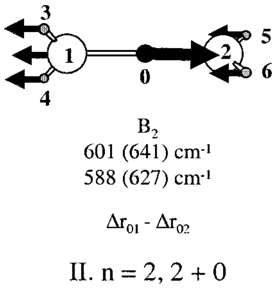

Figure 3. Schematic representations of normal vibration mode having a lithium isotopic shift for $[Li(H_2O)_2]^+$. See the caption description for Figure 2.

means of the root mean square methods. The validity of the basis set super position error (BSSE)[22] of the present approximation was examined in previous works.[18−21] The program used is a GAUSSIAN 98 package.[23]

TABLE 4: Normal Vibration Frequencies $\tilde{\nu}$ (cm^{-1}) of $[Li(H_2O)_3]^+$ with ^{6}Li and ^{7}Li Using Various Calculation Methods III: $n = 3, 3 + 0$ (D_3), $\Gamma_{vib} = 4A_1 + 4A_2 + 8E$

	method[a]					
	A			B		
mode[b]	$\tilde{\nu}_{^6Li}$	$\tilde{\nu}_{^7Li}$	$\Delta\tilde{\nu}^c$	$\tilde{\nu}_{^6Li}$	$\tilde{\nu}_{^7Li}$	$\Delta\tilde{\nu}^c$
E	65	64	1	69	68	1
E	83	83		83	83	
A_2	113	107	6	114	108	6
A_1	173	173		171	171	
A_1^d	232	232		227	227	
A_2	323	323		327	327	
E	329	329		337	337	
E	416	410	6	403	398	5
A_2	465	459	4	452	447	5
E	561	534	27	545	519	26
E	1640	1640		1573	1573	
A_1	1643	1643		1576	1576	
E	3619	3619		3631	3631	
A_1	3623	3623		3635	3635	
A_2	3704	3704		3718	3718	
E	3705	3705		3718	3718	

[a] These various calculation methods are (A) RHF/6-31+G(d) and (B) RHF/6-31++G(d,p), scaled by 0.8964 and 0.8841, respectively. [b] Schematic representations of normal vibration modes are shown. [c] Values give differences of frequencies for two isotopes. [d] Values for A_1 show mode for totally symmetric stretching of Li−O.

TABLE 5: Normal Vibration Frequencies $\tilde{\nu}$ (cm^{-1}) of $[Li(H_2O)_4]^+$ with ^{6}Li and ^{7}Li Using Various Calculation Methods IVa: $n = 4, 4 + 0$ (S_4), $\Gamma_{vib} = 8A + 9B + 8E$

	method[a]					
	A			B		
mode[b]	$\tilde{\nu}_{^6Li}$	$\tilde{\nu}_{^7Li}$	$\Delta\tilde{\nu}^c$	$\tilde{\nu}_{^6Li}$	$\tilde{\nu}_{^7Li}$	$\Delta\tilde{\nu}^c$
E	37	36	1	44	44	
B	42	42		46	46	
A	48	48		56	56	
B	95	95		97	96	1
E	127	127		123	123	
A	129	129		128	128	
A^d	215	215		210	210	
B	217	217		211	211	
E	262	262		275	275	
A	265	265		277	277	
B	312	312		321	320	
E	338	332	6	331	324	7
B	367	359	8	359	351	8
A	389	389		381	381	
E	505	484	21	493	473	20
B	513	494	19	502	483	19
B	1632	1632		1565	1565	
E	1633	1633		1566	1566	
A	1638	1638		1570	1570	
E	3632	3632		3644	3644	
B	3632	3632		3644	3644	
A	3636	3636		3648	3648	
A	3722	3722		3736	3736	
E	3723	3723		3736	3736	
B	3723	3723		3736	3736	

[a] These various calculation methods are (A) RHF/6-31+G(d) and (B) RHF/6-31++G(d,p), scaled by 0.8964 and 0.8841, respectively. [b] Schematic representations of normal vibration modes are shown. [c] Values give differences of frequencies for two isotopes. [d] Values for A show mode for totally symmetric stretching of Li−O.

Results and Discussion

Stable Structure of $[Li(H_2O)_n]^+$. The optimized structures of $[Li(H_2O)_n]^+$ for $n = 1-6$ are shown in Figure 1 with their hydration number. At the same time, the number of water molecules in each cluster is denoted, as $p + q (p + q = n)$, where p and q are in the first and second hydration shells, respectively. Their point groups are also shown under each structural illustration. The optimized structures were obtained in this work with the RHF/6-31+G(d), RHF/6-31++G(d,p), RHF/6-311+G(d), and MP2/6-31+G(d) methods. All of the structures were confirmed to have real harmonic frequencies at the RHF/6-31+G(d) and RHF/6-31++G(d,p) levels. At the

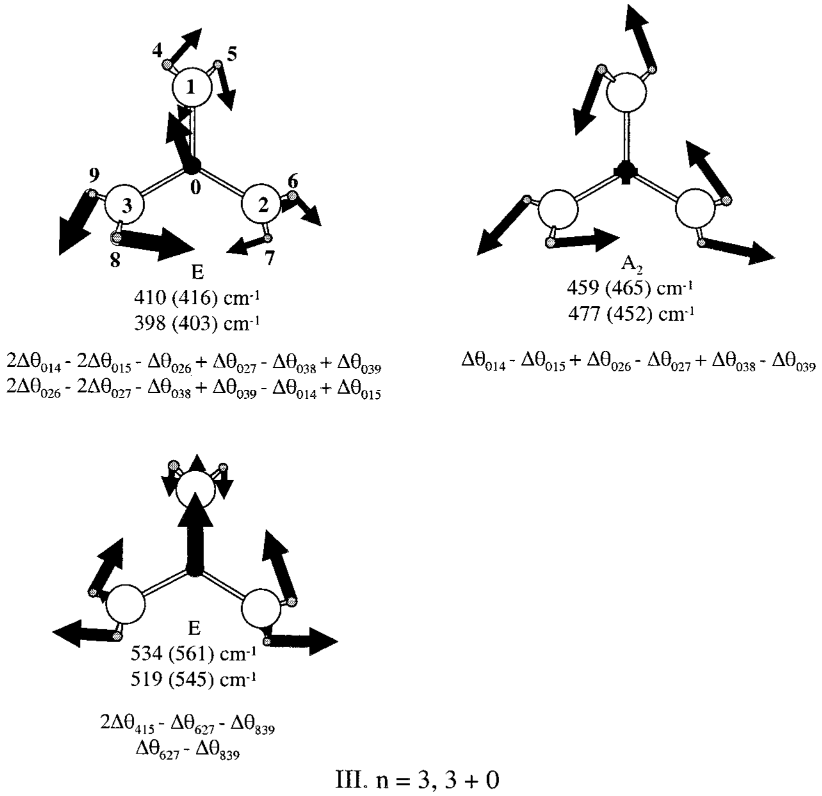

E
410 (416) cm^{-1}
398 (403) cm^{-1}

$2\Delta\theta_{014} - 2\Delta\theta_{015} - \Delta\theta_{026} + \Delta\theta_{027} - \Delta\theta_{038} + \Delta\theta_{039}$
$2\Delta\theta_{026} - 2\Delta\theta_{027} - \Delta\theta_{038} + \Delta\theta_{039} - \Delta\theta_{014} + \Delta\theta_{015}$

A_2
459 (465) cm^{-1}
477 (452) cm^{-1}

$\Delta\theta_{014} - \Delta\theta_{015} + \Delta\theta_{026} - \Delta\theta_{027} + \Delta\theta_{038} - \Delta\theta_{039}$

E
534 (561) cm^{-1}
519 (545) cm^{-1}

$2\Delta\theta_{415} - \Delta\theta_{627} - \Delta\theta_{839}$
$\Delta\theta_{627} - \Delta\theta_{839}$

III. n = 3, 3 + 0

Figure 4. Schematic representations of normal vibration modes having lithium isotopic shifts for $[\text{Li(H}_2\text{O)}_3]^+$. See the caption description for Figure 2.

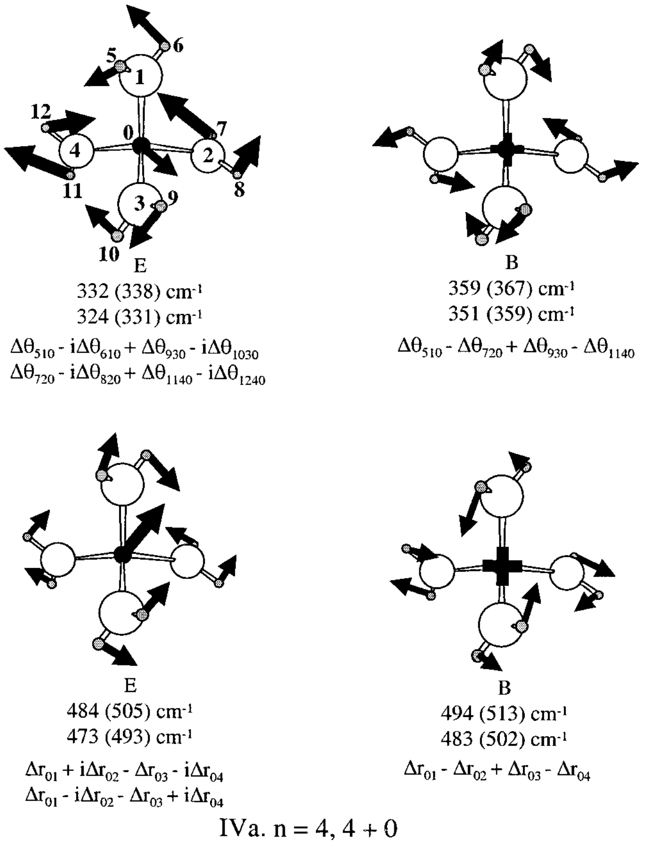

E
332 (338) cm^{-1}
324 (331) cm^{-1}

$\Delta\theta_{510} - i\Delta\theta_{610} + \Delta\theta_{930} - i\Delta\theta_{1030}$
$\Delta\theta_{720} - i\Delta\theta_{820} + \Delta\theta_{1140} - i\Delta\theta_{1240}$

B
359 (367) cm^{-1}
351 (359) cm^{-1}

$\Delta\theta_{510} - \Delta\theta_{720} + \Delta\theta_{930} - \Delta\theta_{1140}$

E
484 (505) cm^{-1}
473 (493) cm^{-1}

$\Delta r_{01} + i\Delta r_{02} - \Delta r_{03} - i\Delta r_{04}$
$\Delta r_{01} - i\Delta r_{02} - \Delta r_{03} + i\Delta r_{04}$

B
494 (513) cm^{-1}
483 (502) cm^{-1}

$\Delta r_{01} - \Delta r_{02} + \Delta r_{03} - \Delta r_{04}$

IVa. n = 4, 4 + 0

Figure 5. Schematic representations of normal vibration modes having lithium isotopic shifts for $[\text{Li(H}_2\text{O)}_4]^+$, IVa (4 + 0). See the caption description for Figure 2.

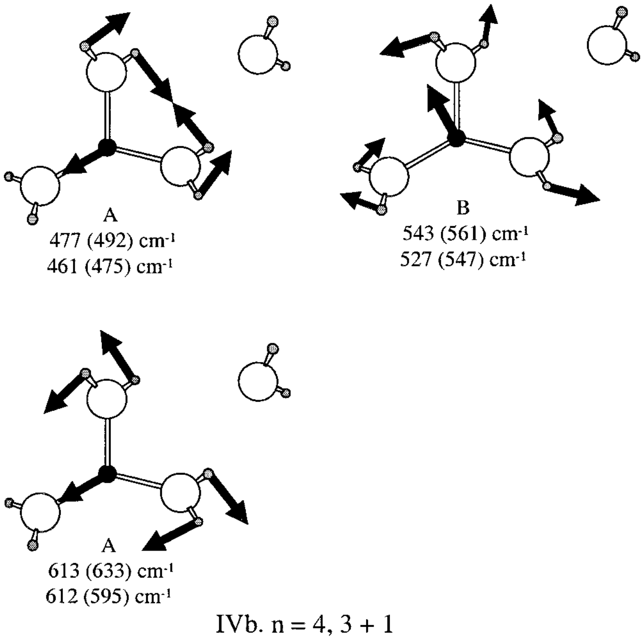

A
477 (492) cm^{-1}
461 (475) cm^{-1}

B
543 (561) cm^{-1}
527 (547) cm^{-1}

A
613 (633) cm^{-1}
612 (595) cm^{-1}

IVb. n = 4, 3 + 1

Figure 6. Schematic representations of normal vibration modes having lithium isotopic shifts for $[\text{Li(H}_2\text{O)}_4]^+$, IVb (3 + 1). The wave numbers (upper line, calculated by the RHF/6-31+G(d) level; lower line, calculated by the RHF/6-31++G(d,p) level), are the data for ^{7}Li (the data for ^{6}Li) after scaling each value (0.8964 for the RHF/6-31+G(d) level, 0.8841 for the RHF/6-31+G(d) level).

RHF/6-311+G(d)level, however, the symmetry of VIa (6 + 0) structure had to be reduced from S_6 to C_1 to obtain real harmonic frequencies. At the MP2/6-31+G(d) level, furthermore, the symmetries of IVa (4 + 0) and Vb (5 + 0) structures had to be reduced to obtain real harmonic frequencies; from S_4 to C_1 for IVa (4 + 0) and from C_2 to C_1 for Vb (5 + 0).

The optimized structures of $[\text{Li(H}_2\text{O)}_n]^+$ for $n = 1-3$ were similar to those in previous reports.[19,20] In the structures ($n \leq$

TABLE 6: Normal Vibration Frequencies $\tilde{\nu}$ (cm^{-1}) of $[Li(H_2O)_4]^+$ with ^6Li and ^7Li Using Various Calculation Methods VIIb: $n = 4$, 3 + 1 (C_2), $\Gamma_{vib} = 16A + 17B$

	method[a]					
	A			B		
mode[b]	$\tilde{\nu}_{^6Li}$	$\tilde{\nu}_{^7Li}$	$\Delta\tilde{\nu}$[c]	$\tilde{\nu}_{^6Li}$	$\tilde{\nu}_{^7Li}$	$\Delta\tilde{\nu}$[c]
B	35	35		35	35	
A	41	41		32	32	
B	61	61		62	62	
A	113	112	1	108	108	
B	119	119		108	108	1
B	145	138	7	141	134	9
A	184	184		171	171	
B	227	226	1	227	227	
A	228	228		226	226	
A	243	243		238	238	
A	246	246		243	243	
B	249	249		254	254	1
B	313	313		318	318	
B	397	394	3	394	391	4
B	425	418	7	421	415	6
B	459	455	4	451	447	4
A	492	477	15	475	461	15
A	534	533	1	518	517	1
B	561	543	18	547	527	20
B	610	609	1	595	591	4
A	633	613	20	612	595	17
B	1626	1626		1556	1556	
A	1627	1627		1557	1557	
A	1641	1641		1574	1574	
A	1656	1656		1583	1583	
B	3559	3559		3568	3568	
A	3574	3574		3582	3582	
A	3619	3619		3631	3631	
A	3623	3623		3636	3636	
B	3704	3704		3716	3716	
B	3706	3706		3720	3720	
A	3708	3708		3719	3719	
B	3708	3708		3722	3722	

[a] These various calculation methods are (A) RHF/6-31+G(d) and (B) RHF/6-31++G(d,p), scaled by 0.8964 and 0.8841, respectively. [b] Schematic representations of normal vibration modes are shown. [c] Values give differences of frequencies for two isotopes.

TABLE 7: Normal Vibration Frequencies $\tilde{\nu}$ (cm^{-1}) of $[Li(H_2O)_5]^+$ with ^6Li and ^7Li Using Various Calculation Methods Va: $n = 5$, 5 + 0 (C_2), $\Gamma_{vib} = 21A + 21B$

	method[a]					
	A			B		
mode[b]	$\tilde{\nu}_{^6Li}$	$\tilde{\nu}_{^7Li}$	$\Delta\tilde{\nu}$[c]	$\tilde{\nu}_{^6Li}$	$\tilde{\nu}_{^7Li}$	$\Delta\tilde{\nu}$[c]
A	30	30		31	31	
A	41	40	1	40	40	
B	41	41		48	48	
B	54	54		59	59	
B	91	90	1	79	77	2
A	100	99	1	99	98	1
B	115	115		112	111	1
A	117	117		112	112	
A	134	134		131	131	
B	168	168		168	168	
B	192	190	2	177	175	2
A[d]	202	202		196	196	
A	217	217		210	210	
B	228	226	2	222	220	2
A	233	233		239	239	
B	248	248		250	250	
A	248	248		249	249	
B	269	269		276	276	
A	293	287	6	287	281	6
B	295	293	2	294	292	2
B	352	348	4	346	342	4
A	356	356		342	342	
B	384	383	1	376	376	
A	397	397		390	390	
A	465	448	17	455	440	15
B	466	455	11	450	438	12
B	500	476	24	486	463	23
B	1616	1616		1546	1546	
A	1618	1618		1548	1548	
A	1623	1623		1554	1554	
B	1625	1625		1555	1555	
A	1627	1627		1558	1558	
B	3637	3637		3648	3648	
A	3637	3637		3648	3648	
A	3639	3639		3650	3650	
B	3648	3648		3658	3658	
A	3650	3650		3659	3659	
B	3732	3732		3744	3744	
A	3733	3733		3744	3744	
B	3733	3733		3746	3746	
A	3746	3746		3757	3757	
B	3746	3746		3758	3758	

[a] These various calculation methods are (A) RHF/6-31+G(d) and (B) RHF/6-31++G(d,p), scaled by 0.8964 and 0.8841, respectively. [b] Schematic representations of normal vibration modes are shown. [c] Values give differences of frequencies for two isotopes. [d] Values for A show mode for totally symmetric stretching of Li−O.

3), all the H_2O molecules are bound directly to Li^+ without hydrogen bonds. For the $[Li(H_2O)_4]^+$ system, two structures are obtained: a IVa (4 + 0) structure, where four H_2O molecules are bound directly to Li^+ without hydrogen bonds, and a IVb (3 + 1) structure, where one H_2O molecule is bound to $[Li(H_2O)_3]^+$ by two hydrogen bonds. This IVb (3 + 1) structure agrees well with that reported by Feller et al.[18,19] For the $[Li(H_2O)_5]^+$ system, a Va (5 + 0) structure, where five H_2O molecules are bound directly to Li^+ without hydrogen bonds, and a Vb (4 + 1) structure, where one H_2O molecule is bound to $[Li(H_2O)_4]^+$ by two hydrogen bonds, are obtained. These are similar to those in previous reports.[18,19,21] For the $[Li(H_2O)_6]^+$ system, one structure, VIa (6 + 0), where all H_2O molecules are bound directly to Li^+ without hydrogen bonds, and two structures; VIb (4 + 2) and VIc(4 + 2), in each of which two H_2O molecules are bound to $[Li(H_2O)_4]^+$ by four hydrogen bonds, are obtained, similar to those in previous reports.[19,21]

The bond lengths between lithium atoms and oxygen atoms (R_{LiO}) of the water molecule in the first hydration shell, and the hydrogen bond lengths (R_{OH}), are summarized in Table 1. The R_{LiO} obtained by the MP2 method are longer than those calculated by the RHF methods irrespective of the basis sets. On the other hand, the R_{OH} calculated by the MP2 method are shorter than those calculated by the RHF methods. The contribution from the energy of the hydrogen bond between water molecules to the total energy seems to be too strong in the MP2 method, since the calculated hydrogen bond lengths, around 1.94−1.98 Å are rather shorter than the well − known value (2.7 Å).[24] In the (n + 0) isomer type, R_{LiO} increases with the increment of the cluster size n. R_{LiO} for the IV (4 + 0) structure is 1.969 Å at the RHF/6-31+G(d) and RHF/6-31++G(d,p) levels. In the VIa (6 + 0) structure, R_{LiO} are 2.150 and 2.158 Å at the RHF/6-31+(d) and RHF/6-31++G(d,p) levels, respectively. These results agree with the experimental values of R_{LiO}; 1.9 Å for a nearest-neighbor number of around 4, and 2.1 Å for the number of around 6.[15] In contrast, R_{LiO} for the most stable isomers, (4 + q) system ($q = 0$, 1, and 2), is saturated around 1.95−1.97 Å.

The hydration energy of the $[Li(H_2O)_n]^+$ system was evaluated using the following reaction:

$$[Li(H_2O)_{n-1}]^+ + H_2O \rightarrow [Li(H_2O)_n]^+ \qquad (7)$$

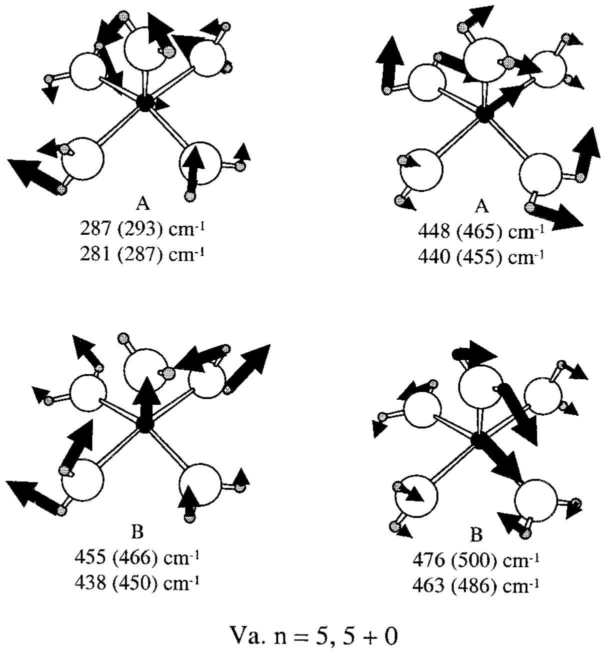

Figure 7. Schematic representations of normal vibration modes having lithium isotopic shifts for $[Li(H_2O)_5]^+$, Va (5 + 0). See the caption description for Figure 6.

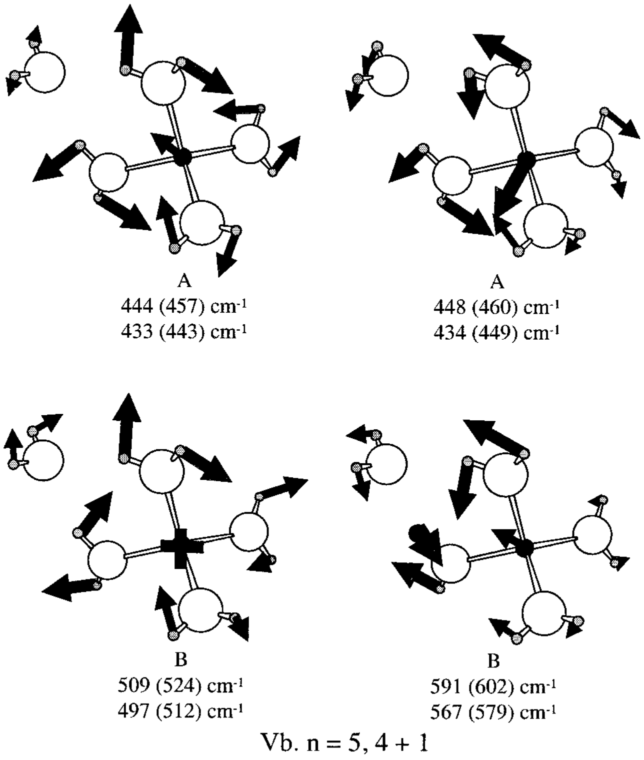

Figure 8. Schematic representations of normal vibration modes having lithium isotopic shifts for $[Li(H_2O)_5]^+$, Vb (4 + 1). See the caption description for Figure 6.

The hydration energy $-\Delta E_n$ for reaction 7 is given as follows:

$$-\Delta E_n = E_{[Li(H_2O)_n]^+} - E_{[Li(H_2O)_{n-1}]^+} - E_{H_2O} \qquad (8)$$

where $E_{[Li(H_2O)_n]^+}$, $E_{[Li(H_2O)_{n-1}]^+}$, and E_{H_2O} are the total energies of $[Li(H_2O)_n]^+$, $[Li(H_2O)_{n-1}]^+$, and H_2O, respectively. The values of $-\Delta E_n$ are shown in Table 1. Moreover, the relative energy differences Δe_n were calculated against each of the most stable isomers of $[Li(H_2O)_n]^+$ (n = 4−6).

TABLE 8: Normal Vibration Frequencies $\tilde{\nu}$ (cm^{-1}) of $[Li(H_2O)_5]^+$ with ^{6}Li and ^{7}Li Using Various Calculation Methods Vb: $n = 5, 4 + 1$ (C_2), $\Gamma_{vib} = 21A + 21B$

	method[a]					
	A			B		
mode[b]	$\tilde{\nu}_{^6Li}$	$\tilde{\nu}_{^7Li}$	$\Delta\tilde{\nu}$[c]	$\tilde{\nu}_{^6Li}$	$\tilde{\nu}_{^7Li}$	$\Delta\tilde{\nu}$[c]
B	26	26		23	22	1
A	52	52		54	54	
A	63	63		65	65	
B	65	64		65	65	
B	100	99	1	99	98	1
B	105	104	1	94	94	
A	125	124	1	121	120	1
B	133	133		125	124	1
A	172	172		164	164	
A	190	190		178	178	
B	209	209		214	214	
A	217	217		211	211	
A	223	223		218	218	
A	228	228		220	220	
B	243	242	1	240	240	
B	274	273	1	275	274	1
A	296	296		297	297	
B	338	332	4	327	322	5
B	354	348	6	350	343	7
A	372	365	7	360	354	6
B	402	394	8	404	396	8
A	457	444	13	443	433	10
B	460	448	12	449	434	15
A	510	505	5	493	489	4
B	524	509	15	512	497	15
B	602	591	11	579	567	12
A	602	600	2	585	584	1
A	1625	1625		1556	1556	
B	1627	1627		1557	1557	
B	1629	1629		1561	1561	
A	1632	1632		1564	1564	
A	1658	1658		1585	1585	
B	3577	3577		3584	3584	
A	3590	3590		3597	3597	
A	3623	3623		3636	3636	
B	3636	3636		3648	3648	
A	3638	3638		3650	3650	
B	3711	3711		3725	3725	
B	3713	3713		3726	3726	
A	3716	3716		3728	3728	
B	3728	3728		3742	3742	
A	3729	3729		3742	3742	

[a] These various calculation methods are (A) RHF/6-31+G(d) and (B) RHF/6-31++G(d,p), scaled by 0.8964 and 0.8841, respectively. [b] Schematic representations of normal vibration modes are shown. [c] Values give differences of frequencies for two isotopes.

Independent of the calculation method, up to $n = 4$, the value of $-\Delta E_n$ tends to become smaller with increasing n. For (n + 0) isomer type, $-\Delta E_5$ of Va (5 + 0) is considerably smaller against $-\Delta E_4$ for IVa (4 + 0), and $-\Delta E_n$ for Va (5 + 0) while VIa (6 + 0) became nearly constant. In contrast, for (4 + q) isomer type, the increment of $-\Delta E_n$ is saturated in the most stable isomers of Vb (4 + 1), VIb (4 + 2), and VIc (4 + 2). The saturation is attributed to water molecules forming a second hydration shell. The present results are the same as those previously published.[21] For the $[Li(H_2O)_4]^+$ system, the IVa (4 + 0) structure is more stable than the IVb (3 + 1) structure by Δe = 8.6 kJ/mol (RHF/6-31+G(d) level) or Δe = 9.9 kJ/mol (RHF/6-31++G(d,p) level). For the $[Li(H_2O)_5]^+$ system, the Vb (4 + 1) structure is more stable than the Va (5 + 0) structure by about Δe = 23 kJ/mol (both calculation levels). For the $[Li(H_2O)_6]^+$ system, the VIb (4 + 2) structure is more stable than the VIa (6 + 0) structure and the VIc (4 + 2) by Δe = 40.9 kJ/mol (RHF/6-31+G(d) level) or Δe = 43.2 kJ/

TABLE 9: Normal Vibration Frequencies $\tilde{\nu}$ (cm^{-1}) of [Li(H$_2$O)$_6$]$^+$ with ^{6}Li and ^{7}Li Using Various Calculation Methods VIa: $n = 6$, 6 + 0 (S_6), $\Gamma_{vib} = 8A_g + 8E_g + 9A_u + 9E_u$

	method[a]					
	A			B		
mode[b]	$\tilde{\nu}_{^6Li}$	$\tilde{\nu}_{^7Li}$	$\Delta\tilde{\nu}$[c]	$\tilde{\nu}_{^6Li}$	$\tilde{\nu}_{^7Li}$	$\Delta\tilde{\nu}$[c]
A_u	58	58		55	55	
Eu	79	79		76	76	
E_g	82	82		75	75	
A_g	93	93		89	89	
A_u	113	111	2	106	104	2
E_g	120	120		113	113	
E_u	127	127		123	123	
E_u	190	188	2	192(195)	188(191)	4
A_g[d]	192	192		182	182	
E_g	230	229	1	228	227(228)	1(0)
A_u	233	230	3	219	215	4
E_u	245	239	6	230	224(226)	6(4)
A_g	266	266		260	260	
E_g	275	275	275	267(265)	267(265)	
A_u	296	296		290	290	
E_u	315	312	3	299	298	1
A_g	352	352		330	330	
E_g	406	406		389(391)	389(391)	
A_u	465	465		443	441	2
A_g	479	479		462	462	
E_u	481	471	10	461	451	10
A_u	506	487	19	479	452	27
A_g	1613	1613		1540	1540	
E_u	1615	1615		1542	1542	
A_u	1617	1617		1543	1543	
E_g	1620	1620		1546	1546	
A_u	3633	3633		3645	3645	
E_g	3636	3636		3648	3648	
A_g	3637	3637		3648	3648	
E_u	3638	3638		3649	3649	
A_g	3735	3735		3748	3748	
A_u	3736	3736		3749	3749	
E_g	3736	3736		3749	3749	
E_u	3736	3736		3749	3749	

[a] These various calculation methods are (A) RHF/6-31+G(d) and (B) RHF/6-31++G(d,p), scaled by 0.8964 and 0.8841, respectively. [b] Schematic representations of normal vibration modes are shown. [c] Values give differences of frequencies for two isotopes. [d] Values for A_g show mode for totally symmetric stretching of Li−O.

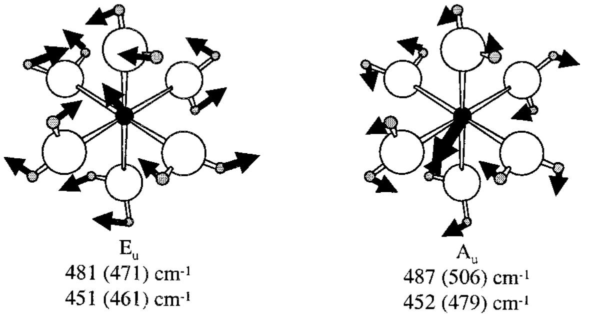

Figure 9. Schematic representations of normal vibration modes having lithium isotopic shifts for [Li(H$_2$O)$_6$]$^+$, VIa (6 + 0). See the caption description for Figure 6.

mol (at the RHF/6-31++G(d,p) level) and $\Delta e = 7.0$ kJ/mol (RHF/6-31+G(d) level) or $\Delta e = 7.3$ kJ/mol (RHF/6-31++G(d,p) level), respectively. These suggest that four water molecules bound directly to the central lithium atom form the most stable structure in the first hydration shell.

TABLE 10: Normal Vibration Frequencies $\tilde{\nu}$ (cm^{-1}) of [Li(H$_2$O)$_6$]$^+$ with ^{6}Li and ^{7}Li Using Various Calculation Methods Vlb: $n = 6$, 4 + 2 ($D_{2,1}$), $\Gamma_{vib} = 7A_1 + 5A_2 + 6B_1 + 7B_2 + 13E$

	method[a]					
	A			B		
mode[b]	$\tilde{\nu}_{^6Li}$	$\tilde{\nu}_{^7Li}$	$\Delta\tilde{\nu}$[c]	$\tilde{\nu}_{^6Li}$	$\tilde{\nu}_{^7Li}$	$\Delta\tilde{\nu}$[c]
E	32	32		31	31	
B_1	33	33		39	39	
E	87	87		84	84	
A_1	89	89		85	85	
B_2	110	110		117	116	1
E	124	124		116	116	
B_2	151	150	1	143	142	1
E	181	181		192	192	
A_1	184	184		170	170	
B_2	188	188		176	175	1
A_2	205	205		203	203	
A_2	217	217		207	207	
E	225	225		218	218	
A_1	229	229		223	223	
A_1	246	246		237	237	
E	342	336	6	337	330	7
E	396	388	8	396	389	7
B_1	422	406	16	406	391	15
E	482	471	11	470	459	11
A_2	494	494		477	477	
B_1	495	495		478	478	
A_1	522	522		499	499	
E	589	588	1	573	572	1
B_2	616	599	17	592	575	17
E	1627	1627		1551	1551	
B_2	1630	1630		1553	1553	
A_1	1631	1631		1555	1555	
B_2	1661	1661		1581	1581	
A_1	1662	1662		1582	1582	
E	3602	3602		3595	3595	
B_2	3612	3612		3604	3604	
A_1	3617	3617		3610	3610	
B_2	3641	3641		3639	3639	
A_1	3641	3641		3639	3639	
E	3729	3729		3730	3730	
E	3737	3737		3733	3733	
A_1	3740	3740		3737	3737	
B_2	3741	3741		3737	3737	

[a] These various calculation methods are (A) RHF/6-31+G(d) and (B) RHF/6-31++G(d,p), scaled by 0.8964 and 0.8841, respectively. [b] Schematic representations of normal vibration modes are shown. [c] Values give differences of frequencies for two isotopes.

In summary, no significant difference was seen in the structures and the binding energies among the four present calculation levels, although the MP2/6-31+G(d) method gave a somewhat larger estimation of the binding energies. These calculations are also well correlated with the experimental results; X-ray and neutron diffraction analyses have given mostly a coordination number of four and R_{LiO} of 1.96 Å although the coordination number and R_{LiO} vary from 3.3 to 6.5 and from 1.9 to 2.1 Å, respectively.[25−27]

Normal Vibration Analysis of [Li(H$_2$O)$_n$]$^+$ with Isotopic Shifts. The normal vibration frequencies of the [Li(H$_2$O)$_n$]$^+$ clusters were obtained for each lithium isotope through the normal vibration analyses of the optimized structures (Tables 2−11). All real vibration frequencies were obtained for the RHF/6-31+G(d) level and the RHF/6-31++G(d,p) level. The normal vibration modes were analyzed using group theory and the irreducible representations were derived, as are shown in each table. For the small clusters such as the I, II, III and IVa structures, the potential could be expressed by the internal coordinates and the normal vibration mode could be identified definitively. The vibration modes having great isotopic shifts are shown schematically in Figures 2−11.

For cluster I with (1 + 0) structure, a large isotopic shift, $\Delta\tilde{\nu} = 29$ cm^{-1}, appears around 500 cm^{-1}: 500 (529) cm^{-1} (the

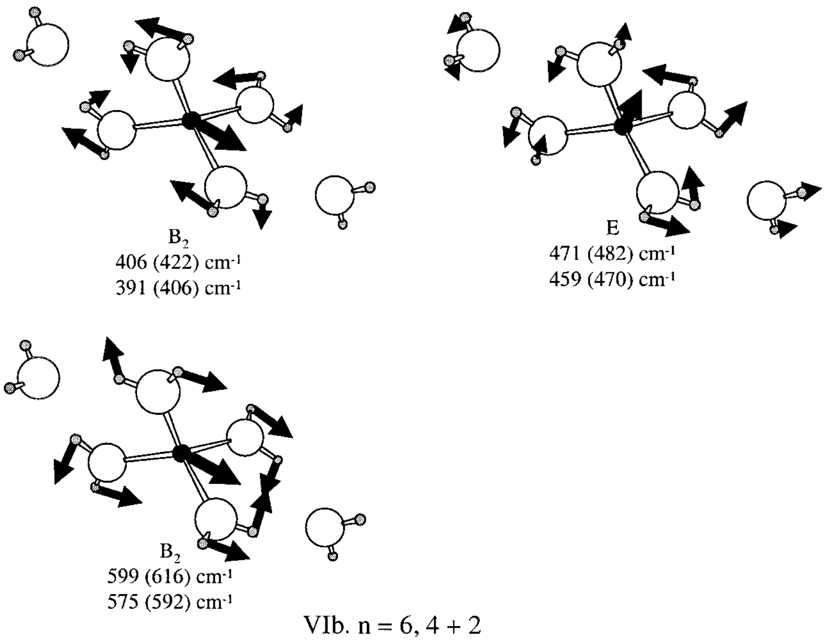

Figure 10. Schematic representations of normal vibration modes having lithium isotopic shifts for $[Li(H_2O)_6]^+$, VIb (4 + 2). See the caption description for Figure 6.

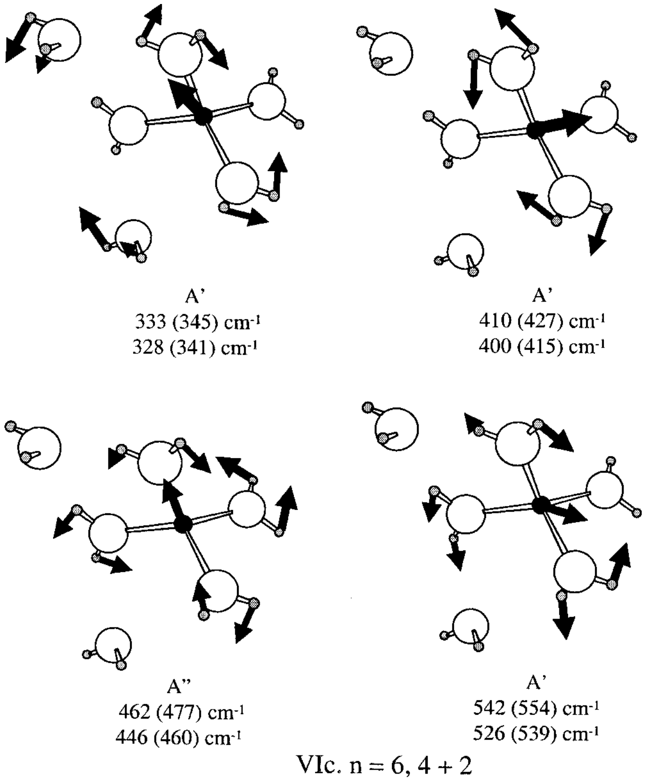

Figure 11. Schematic representations of normal vibration modes having lithium isotopic shifts for $[Li(H_2O)_6]^+$, VIc (4 + 2). See the caption description for Figure 6.

numbers correspond to the wave numbers for ^{7}Li clusters while those in parentheses refer to the wave numbers for ^{6}Li clusters) by the RHF/6-31+G(d) level and 491 (520) cm^{-1} by the RHF/6-31++G(d,p) level (Table 2). The frequency mode can be assigned to A_1 mode; that is a stretching vibration of the bond between a lithium atom and an H_2O molecule, as shown in Figure 2. For cluster II with (2 + 0) structure, a large isotopic shift of about $\Delta\tilde{\nu} \simeq 40$ cm^{-1} appears around 600 cm^{-1}: 601 (641) cm^{-1} by the RHF/6-31+G(d) level and 588 (627) cm^{-1} by the RHF/6-31++G(d,p) level (Table 3). The frequency mode can be assigned to B_2 mode; that is Li-O stretching vibrations (see Figure 3). For cluster III with (3 + 0) structure, large isotopic shifts, $\Delta\tilde{\nu} = 27$ or 26 cm^{-1}, appears at 500−550 cm^{-1}: 534 (561) cm^{-1} by the RHF/6-31+G(d) level and 519 (545) cm^{-1} by the RHF/6-31++G(d,p) level (Table 4). The frequency mode can be assigned to E modes; these are coupling modes consisting of Li−O asymmetrically stretching vibrations and the rocking vibrations of two H_2O molecules. The other frequency modes having an isotopic shift correspond to coupling vibrations, which consist of the asymmetic vibration of the central lithium atom relative to the surrounding water molecules and the rocking vibrations of the three H_2O molecules (see Figure 4). For clusters IVa with (4 + 0) structure, large isotopic shifts, $\Delta\tilde{\nu} \simeq 20$ cm^{-1}, appear around 500 cm^{-1} at both calculation levels (Table 5). The largest isotopic shift appears at 484 (505) cm^{-1} at the RHF/6-31+G(d) level and 473 (493) cm^{-1} at the RHF/6-31++G(d,p) level, which can be assigned to E modes. A very large isotopic shift appears at 494 (513) cm^{-1} at the RHF/6-31+G(d) level and 483 (502) cm^{-1} at the RHF/6-31++G(d,p) level, which can be assigned to B mode. Both consist of the assymetrical stretching vibrations of Li−O bonds relative to the surrounding four H_2O molecules, combined with the weak rocking vibrations of the four H_2O molecules (see Figure 5). The other frequency modes have small isotopic shifts $\Delta\tilde{\nu} < 10$ cm^{-1}, which appear at around 330−360 cm^{-1}, and are ascribed to the coupling vibrations between the weak Li-O stretching vibrations (or the O−Li−O scissoring vibrations) and the rocking vibrations of the H_2O molecules (see Figure 5). For cluster IVb with a (3 + 1) structure, very large isotopic shifts, $\Delta\tilde{\nu} = 15-20$ cm^{-1}, appear at 477 (492), 543 (561), and 613 (633) cm^{-1} at the RHF/6-31+G(d) level, and 461 (475), 527 (545) and 595 (612) cm^{-1} at the RHF/6-31++G-(d,p) level, which can be assigned to modes A, and B and B, respectively (Table 6). All these frequency modes consist of the asymmetrical stretching vibrations of Li-O bonds relative to the surrounding three H_2O molecules, combined with the rocking vibrations of the three H_2O molecules in the first hydration shell (see Figure 6). For cluster Va with (5 + 0) structure, large isotopic shifts $\Delta\tilde{\nu} \geq 10$ cm^{-1}, appear around 400−500 cm^{-1} at both calculation levels. The B mode having

TABLE 11: Normal Vibration Frequencies $\tilde{\nu}$ (cm^{-1}) of [Li(H$_2$O)$_6$]$^+$ with ^{6}Li and ^{7}Li Using Various Calculation Methods VIc: $n = 6$, 4 + 2 (C_s), $\Gamma_{vib} = 27A' + 24A''$

	method[a]					
	A			B		
mode[b]	$\tilde{\nu}_{^6\mathrm{Li}}$	$\tilde{\nu}_{^7\mathrm{Li}}$	$\Delta\tilde{\nu}$[c]	$\tilde{\nu}_{^6\mathrm{Li}}$	$\tilde{\nu}_{^7\mathrm{Li}}$	$\Delta\tilde{\nu}$[c]
A″	29	29		26	26	
A′	36	36		34	34	
A′	49	49		50	50	
A″	53	53		57	57	
A′	73	72		67	66	1
A″	109	109		97	97	
A′	116	115	1	111	111	
A″	123	122	1	117	116	1
A″	135	135		127	127	
A′	136	135	1	131	131	
A′	156	155	1	145	145	
A″	187	187		189	189	
A′	198	198		196	196	
A″	206	206		203	203	
A′	206	206		205	205	
A″	214	214		209	209	
A′	219	219		215	215	
A″	238	238		225	225	
A′	238	238		229	229	
A′	267	267		267	267	
A′	345	333	12	341	328	13
A″	349	345	4	337	332	5
A″	352	352		353	353	
A′	381	376	5	384	378	6
A′	427	410	17	415	400	15
A″	433	430	3	422	419	3
A″	477	462	15	460	446	14
A″	487	487		468	468	
A′	492	492		475	475	
A′	554	542	12	539	526	13
A″	568	566	2	552	550	2
A′	601	597	4	579	575	4
A″	646	639	7	612	605	7
A′	1628	1628		1550	1550	
A″	1628	1628		1552	1552	
A′	1630	1630		1554	1554	
A′	1633	1633		1559	1559	
A″	1645	1645		1567	1567	
A′	1664	1664		1582	1582	
A′	3600	3600		3593	3593	
A″	3606	3606		3599	3599	
A′	3614	3614		3606	3606	
A″	3638	3638		3636	3636	
A′	3641	3641		3640	3640	
A′	3657	3657		3655	3655	
A″	3694	3694		3690	3690	
A″	3731	3731		3731	3731	
A′	3731	3731		3731	3731	
A″	3735	3735		3732	3732	
A′	3735	3735		3732	3732	
A″	3752	3752		3750	3750	

[a] These various calculation methods are (A) RHF/6-31+G(d) and (B) RHF/6-31++G(d,p), scaled by 0.8964 and 0.8841, respectively. [b] Schematic representations of normal vibration modes are shown. [c] Values give differences of frequencies for two isotopes.

the largest isotopic shift, $\Delta\tilde{\nu} = 23$ or 24 cm^{-1}, appears at 476 (500) cm^{-1} at the RHF/6-31+G(d) level and 463 (486) cm^{-1} at the RHF/6-31++G(d,p) level and (Table 7). In all these modes, the Li-O stretching vibrations are coupled with the weak rocking vibrations of the surrounding H$_2$O molecules. There are small isotopic shifts at about 300 cm^{-1}. All these frequency modes consist of weak Li−O stretching vibrations or weak O−Li−O scissoring vibrations, and the rocking vibrations of the surrounding H$_2$O molecules (see Figure 7). For cluster Vb with (4 + 1) structure, large isotopic shifts, $\Delta\tilde{\nu} \geq 10$ cm^{-1}, appear around 450 cm^{-1} and 500−600 cm^{-1} at both calculation levels (Table 8). The frequency modes can be assigned to the modes A and B, respectively, which are coupling modesl consisting of Li−O stretching vibrations and the rocking vibrations of the H$_2$O molecules in the first and second hydration shells, respectively (see Figure 8). For cluster VIa with (6 + 0) structure, large isotopic shifts $\Delta\tilde{\nu} \geq 10$ cm^{-1}, appear around 450−500 cm^{-1} at both calculation levels (Table 9). The frequency modes can be assigned to the modes E$_u$ and A$_u$, respectively, which are coupling vibrations consisting of the asymmetic vibration of the lithium atom relative to the surrouding H$_2$O molecules and the rocking vibrations of the H$_2$O molecules, respectively (see Figure 9). For cluster VIb with (4 + 2) structure, a large isotopic shift, $\Delta\tilde{\nu} = 17$ cm^{-1}, appears around 600 cm^{-1}: 599 (616) cm^{-1} at the RHF/6-31+G(d) level and 575 (592) cm^{-1} at the RHF/6-31++G(d,p) level, which can be assigned to the B$_2$ mode (Table 10). Comparatively large isotopic shifts appear at around 400−480 cm^{-1} at both calculation levels, which can be assigned to modes B$_2$ and E, respectively. In each of these modes, the Li−O stretching vibrations or weak O−Li−O scissoring vibrations are coupled with the rocking vibrations of the surrounding H$_2$O molecules. Mode E is the coupling vibration involving the weak rocking vibrations of the H$_2$O molecules in the second hydration shell, but mode B does not involve the vibration of the H$_2$O molecules in the second hydration shell (see Figure 10). E modes having small isotopic shifts, which consist of asymmetrical weak stretching vibrations of Li−O bonds relative to the surrounding H$_2$O molecules combined with the rocking vibrations of the H$_2$O molecules, appear at 300−400 cm^{-1}. For cluster VIc with a (4 + 2) structure, comparatively large isotopic shifts, $\Delta\tilde{\nu} > 10$ cm^{-1}, appear at 333 (345), 410 (427), 462 (477), and 542 (554) cm^{-1} at the RHF/6-31+G(d) level, and 328 (341), 400 (415), 446 (460), and 526 (539) cm^{-1} at the RHF/6-31++G(d,p) level (Table 11). In all these modes, the Li−O stretching vibrations or weak O−Li−O scissoring vibrations are coupled with the rocking vibrations of the surrounding H$_2$O molecules. The modes having isotopic shift correspond almost exactly to the same vibration frequencies at different calculation levels, and the extent of these shifts is almost the same. The above results show that the normal vibration modes in the presence of an isotopic shift vary widely depending on the number of hydrated water molecules and on the mode of hydration. However, we can see a common feature for these modes: they all include the asymmetric vibrations of central lithium atoms relative to the surrounding H$_2$O molecules in the first hydration shell.

TABLE 12: Values of f_n^r

		method	
n	symbol	A[a]	B[b]
(n + 0) system			
1	I	1.030	1.029
2	II	1.051	1.049
3	III	1.067	1.064
4	IVb	1.070	1.066
5	Va	1.056	1.052
6	VIa	1.046	1.041
(3 + p) system			
4	IVa	1.069	1.066
(4 + p) system			
5	Vb	1.071	1.068
6	VIb	1.070	1.067
6	VIc	1.070	1.067

[a] Frequencies used are calculated at RHF/6-31+G(d) with a scale of 0.8964. [b] Frequencies used are calculated at RHF/6-31++G(d,p) with a scale of 0.8841.

TABLE 13: Totally Symmetric Stretching Frequencies of Li−O $\tilde{\nu}_1$ (cm^{-1}), Values of Approximated Reduced Partition Function Ratio $f_n^{r,a}$, and Errors of $f_n^{r,a}$ against f_n^{r}, δ (%)

		method						experiment			
		A[a]			B[b]			ref 13		ref 14	
n	symbol	$\tilde{\nu}_1$	$f_n^{r,a}$	δ	$\tilde{\nu}_1$	$f_n^{r,a}$	δ	$\tilde{\nu}_1$	$f_n^{r,a}$	$\tilde{\nu}_1$	$f_n^{r,a}$
2	II	251	1.046	−0.5	246	1.044	−0.5				
3	III	232	1.059	−0.4	227	1.056	−0.8				
4	IVa	215	1.067	−0.3	210	1.064	−0.2	255	1.095	190	1.053
5	Va	202	1.074	1.7	196	1.070	1.7				
6	VIa	192	1.081	3.3	182	1.072	3.0				

[a] Frequencies used are calculated at RHF/6-31+G(d) with a scale of 0.8964. [b] Frequencies used are calculated at RHF/6-31++G(d,p) with a scale of 0.8841.

f^r of Lithium Ions in Aqueous Solution. For the $[Li(H_2O)_n]^+$ clusters up to $n = 6$, the values of f_n^r at 298 K were calculated for each cluster using eq 4 with the calculated normal vibration frequencies and are shown in Table 12. As mentioned before, the effect of the calculation level is not so significant, and the estimation of f_n^r is carried out at two calculation levels, the RHF/6-31+G(d) and RHF/6-31++G(d,p) levels. In the (n + 0) system, the value of f_n^r increases from 1.030 to 1.070 with an increase up to $n = 4$; the highest value of f_n^r is 1.070 at $n = 4$ at the RHF/6-31+G(d) level; and from 1.029 to 1.066 with an increase up to $n = 4$; the highest value of f_n^r is 1.066 at $n = 4$ at the RHF/6-31++G(d,p) level. For $n = 5$ and 6, the value of f_n^r decreases with n at both calculation levels. The decrease of the f_n^r value with n can be explained by the considerable increase in the Li−O bond length at $n \geq 5$. The increase in the bond length causes a marked decrease of isotopic effect although the number of vibration modes associated with isotopic shift increases with n. It is well-known that the isotopic separation factor between species with different coordination numbers (for example, $SnCl_4 \Leftrightarrow SnCl_6$) is small because the isotopic effect due to the increase in the coordination number is compensated for by the reverse effect due to the increase of bond length.[10] The present results indicate that the isotopic effect due to the increase in the hydration number exceeds that due to the increase in the bond length for clusters with $n \leq 4$, while the reverse is found for clusters with $n \geq 5$.

In the (4 + q) system, the values of f_n^r are 1.071 and 1.070 for $n = 5$ and 6, respectively, at the RHF/6-31+G(d) level; and 1.068 and 1.067 for $n = 5$ and 6, respectively, at the RHF/6-31++G(d,p) level. At both calculation levels, these f_n^r values are close to the f_n^r values for the IVa (4 + 0) system. A slight distortion of the first − shell hydration structure may make the f_n^r value a little larger in the (4 + q) system. These results indicate that the f_n^r values are determined mainly by the first-shell hydration structure, but rarely influenced by the second-shell hydration structure, although the normal vibration modes are apparently influenced by the second-shell water molecules. Since the distance between the central lithium atom and the second-shell water molecules is large, the contribution due to their vibration may be reduced compared to those involving first-shell water molecules. On the other hand, in the $[Li(H_2O)_4]^+$ system, the value of f_n^r for IVa (3 + 1) is close to that of IVa (4 + 0). Although the values of f_n^r are determined mainly by the first-shell hydration structure, the value of f_n^r for IVa (3 + 1) is larger than that of III (3 + 0) since the symmetry of the first-shell hydration structure for IVa (3 + 1) breaks. We can conclude from these calculations that the lithium isotopic effect of hydrated lithium ions arises mainly from the local vibrations between the lithium ions and the first-shell water, while the long-range interaction involving the water molecules far from the first hydration shell can be ignored.

The energy calculations described above show that the hydrated cluster with four water molecules in the first hydration shell is the most stable. Therefore, we can estimate $f_{Li,aq}^r$ to be 1.07 from the f_n^r values of clusters (4 + q). Furthermore, the effects of using scaling factors for the f_n^r values are not so large, although effects to a greater or lesser extent of the scaling factors exist for each frequency. Consequently, the theoretical upper limit of the isotopic separation factor is given as $f_{Li,aq}^r = 1.07$ in the aqueous solution−exchanger system.

Validity of Bigeleisen and Mayer's Rough Approximation for f^r. For the (n + 0) system of the $[Li(H_2O)_n]^+$ clusters ($n = 2-6$), the roughly approximated values for reduced partition function ratio ($f_n^{r,a}$) at 298 K could be calculated from the totally symmetric stretching frequencies, which were calculated at the RHF/6-31+G(d) level and the RHF/6-31++G(d,p) level of the clusters using eq 6. The calculated $f_n^{r,a}$ values are given in Table 13 with their errors against each f_n^r value. In the (n + 0) clusters with $n = 2-4$, the values of $f_n^{r,a}$ with small errors within 0.8% against each f_n^r value agree rather well with the f_n^r values, respectively. In the (n + 0) clusters with $n \geq 5$, although there are discrepancies between the $f_n^{r,a}$ and f_n^r values, the values of $f_n^{r,a}$ are overestimated, and include errors up to 3.3%. The deviation becomes larger with n since the value of $f_n^{r,a}$ increases consistently with n while the f_n^r value decreases in the region $n \geq 4$. The deviation observed in the (6 + 0) cluster can be anticipated due to the influence of the interaction between H_2O molecules due to hydrogen bonds. The geometry of water molecules suggests the formation of weak hydrogen bonds between neighboring H_2O molecules. These hydrogen bonds affect the totally symmetric stretching frequency, but rarely affect the asymmetric vibration frequency of the central lithium atom relative to the surrounding H_2O molecules. These calculations show that Bigeleisen and Mayer's rough approximate formula can be applied for the most stable $[Li(H_2O)_n]^+$ clusters ($n = 2-6$). This makes it possible to compare our calculated data with the isotopic effect estimated from spectroscopic data. The values of $f_n^{r,a}$ derived from the Raman active spectra are also shown in Table 13 assuming a coordination number of 4. Two values, 1.095 and 1.053, are obtained depending on the wavenumbers of Raman bands. These values agree approximately with our calculated values of $f_{Li,aq}^r$, although considerable variation is observed. Further spectroscopic studies will be necessary to confirm our calculations from an experimental standpoint.

Isotopic Separation Factors in the Chemical Exchange Reaction. The present calculations give some useful information, not only on the f^r value of hydrated lithium ions, but also on the isotopic fractionation properties in the chemical exchange reactions. Since the value of $f^{r}_{\mathrm{Li,aq}}$ is constant in the reaction involving an aqueous solution phase, separation factors in the chemical exchange reaction are controlled by the value of the lithium isotopic reduced partition function ratio in the exchanger phase ($S = 1.07/f^{r}_{\mathrm{Li,exch}}$). This means that the maximum separation factor for the lithium isotopic exchange reaction in aqueous solution is 1.07 when separation factor (S) is defined by eq 2; i.e., it involves hydrated lithium ions and ^{7}Li concentrates in the aqueous phase. The experimentally determined separation factors are all less than 1.05. The highest separation factor obtained experimentally is 1.05, which is observed in the lithium−amalgam system.[2] In the lithium−amalgam phase, lithium atoms exist in metal form and are interspersed with mercury atoms randomly. Therefore, the isotopic effect due to the vibration of lithium atoms may be very small in the lithium amalgam system, and consequently may give a small $f^{r}_{\mathrm{Li,exch}}$ value.

The ($n + 0$) type clusters in the present study can be regarded as simple model clusters of lithium compounds in some of the exchanger phases, since lithium ions are usually coordinated by the oxygen atoms of organic ionophores or of inorganic metal oxides. The 4-, 5-, and 6-coordinated structures have been found in these phases.[28,29] We have observed that cubic antimonic acid with 5-coordination sites shows a high separation factor (1.024) for lithium isotopes, while spinel-type manganese oxide with 4-coordination sites does not show any lithium isotopic effect.[4] The isotopic effect due to the change in coordination structure can be roughly evaluated as a ratio of the f^{r}_{n} values since the isotopic effect arises from the local vibration modes of Li^{+}-containing clusters. The change of coordination number from 4 to 5 gives a separation factor of 1.013 and that from 4 to 6 gives a value of 1.024. These calculations suggest that the change of coordination structure is effective for lithium isotope fractionation and plays an important role in isotope fractionation in the chemical exchange reaction. We can design effective separation agents through the calculation of the values for the reduced partition function ratio for solvated lithium ion clusters.

Conclusion

The most stable lithium ion hydrated structure in aqueous solution was determined by the ab initio MO calculation. The normal vibration analyses for the structure of the hydrated lithium gave the reduced partition function ratio of lithium isotopes in an aqueous phase (1.07); this value can be regarded as the maximum for the lithium isotopic separation factor in the aqueous solution/exchanger system. The concept developed in the present study will stimulate the creation of lithium isotope separators with higher functions.

References and Notes

(1) Symons, E. A. *Sep. Sci. Technol.* **1985**, *20*, 633.

(2) Palko, A. A.; Drury, J. S.; Begun, G. M. *J. Chem. Phys.* **1976**, *64*, 1828.

(3) Singh, G.; Hall, J. C.; Rock, P. A. *J. Chem. Phys.* **1972**, *56*, 1855. Singh, G.; Rock, P. A. *J. Chem. Phys.* **1972**, *57*, 5556. Hall, J. C.; Silvester, L. F.; Singh, G.; Rock, P. A. *J. Chem. Phys.* **1973**, *59*, 6358.

(4) Ooi, K.; Feng, Q.; Kanoh, H.; Hirotsu, T.; Oi, T. *Sep. Sci. Technol.* **1995**, *30*, 3761.

(5) Ogino, H.; Oi, T. *Sep. Sci. Tehcnol.* **1996**, *31*, 1215.

(6) Nishizawa, K.; Watanabe, H.; Ishino, S.; Shinagawa, M. *J. Nucl. Sci. Technol.* **1984**, *21*, 133. Nishizawa, K.; Watanabe, H. *J. Nucl. Sci. Technol.* **1986**, *23*, 843. Nishizawa, K.; Takano, T.; Ikeda, I.; Okahara, M. *Sep. Sci. Technol.* **1988**, *23*, 333.

(7) Thomas, M. W.; Mariñas, B. J.; Fritz, S. J. *J. Membr. Sci.* **1994**, *88*, 231.

(8) Ooi, K.; Kanoh, H.; Sugihara, H.; Hiratani, K. *Chem. Lett.* **1997**, 615.

(9) Urey, H. C. *J. Chem. Soc.* **1974**, 562.

(10) Bigeleisen, J.; Mayer, M. G. *J. Chem. Phys.* **1947**, *15*, 261.

(11) Michaelian, K. H.; Moskovits, M. *Nature* **1978**, *273*, 135.

(12) Kanno, H.; Hiraishi, J. *J. Phys. Chem.* **1983**, *87*, 3664.

(13) Kameda, Y.; Ebata, H.; Uemura, O. *Bull. Chem. Soc. Jpn.* **1994**, *67*, 929.

(14) Rudolph, W.; Brooker, M. H.; Pye, C. C. *J. Chem. Phys.* **1995**, *99*, 3793.

(15) Marcus, Y. *Chem. Rev.* **1988**, *88*, 1475.

(16) Ohtaki, H.; Radnai, T. *Chem. Rev.* **1993**, *93*, 1157.

(17) Bischof, G.; Silbernagl, A.; Hermansson, K.; Probst, M. *Int. J. Quantum Chem.* **1997**, *65*, 803.

(18) Feller, D.; Glendening, E. D.; Kendall, R. A.; Peterson, K. A. *J. Chem. Phys.* **1994**, *100*, 4981.

(19) Glendening, E. D.; Feller, D. *J. Phys. Chem.* **1995**, *99*, 3060.

(20) Pye, C. C.: Rudolph, W.; Poirier, R. A. *J. Phys. Chem.* **1996**, *100*, 601.

(21) Hashimoto, K.; Kamimoto, T. *J. Am. Chem. Soc.* **1998**, *120*, 3560.

(22) Boys, S. F.; Bernardi, F. *Mol. Phys.* **1970**, *19*, 533.

(23) Frisch, M. J.; Trucks, G. W.; Schlegel, H. B.; Scuseria, G. E.; Robb, M. A.; Cheeseman, J. R.; Zakrzewski, V. G.; Montgomery, J. A., Jr.; Stratmann, R. E.; Burant, J. C.; Dapprich, S.; Millam, J. M.; Daniels, A. D.; Kudin, K. N.; Strain, M. C.; Farkas, O.; Tomasi, J.; Barone, V.; Cossi, M.; Cammi, R.; Mennucci, B.; Pomelli, C.; Adamo, C.; Clifford, S.; Ochterski, J.; Petersson, G. A.; Ayala, P. Y.; Cui, Q.; Morokuma, K.; Malick, D. K.; Rabuck, A. D.; Raghavachari, K.; Foresman, J. B.; Cioslowski, J.; Ortiz, J. V.; Stefanov, B. B.; Liu, G.; Liashenko, A.; Piskorz, P.; Komaromi, I.; Gomperts, R.; Martin, R. L.; Fox, D. J.; Keith, T.; Al-Laham, M. A.; Peng, C. Y.; Nanayakkara, A.; Gonzalez, C.; Challacombe, M.; Gill, P. M. W.; Johnson, B.; Chen, W.; Wong, M. W.; Andres, J. L.; Gonzalez, C.; Head-Gordon, M.; Replogle, E. S.; Pople, J. A. *GAUSSIAN 98*, Revision A.6; Gaussian, Inc.: Pittsburgh, PA, 1998.

(24) Kuleshova, L. N.; Zorkii, P. M. *Acta Crystallogr.* **1981**, *B37*, 1363.

(25) Enderby, J. E.; Neilson, G. W. *Adv. Phys.***1980**, *29*, 323.

(26) Yamanaka, K.; Yamagami, M.; Takamuku, T.; Yamaguchi, T.; Wakita, H. *J. Phys. Chem.* **1993**, *97*, 10835. Yamagami, M.; Yamaguchi, T.; Wakita, H.; Misawa, M. *J. Chem. Phys.* **1994**, *100*, 3122.

(27) Kameda, Y.; Uemura, O. *Bull. Chem. Soc. Jpn.* **1993**, *66*, 384. Kameda, Y.; Ebata, H.; Usuki, T.; Uemura, O. *Phys. B* **1995**, *213 & 214*, 477. Kameda, Y.; Suzuki, S.; Ebata, H.; Usuki, T.; Uemura, O. *Bull. Chem. Soc. Jpn.* **1997**, *70*, 47. Kameda, Y.; Usuki, T.; Uemura, O. *High Temp. Mater. Processes* **1999**, *18*, 27.

(28) Wenger, M.; Armbruster, Th. *Eur. J. Mineral.* **1991**, *3*, 387.

(29) Olsher, U.; Izatt, R. M.; Bradshaw, J. S.; Dalley, N. K. *Chem. Rev.* **1991**, *91*, 137.